Control of Product Quality in Polymerization Processes

Francis J. Doyle III
Department of Chemical Engineering
University of Delaware
Newark, DE 19716

Masoud Soroush
Department of Chemical Engineering
Drexel University
Philadelphia, PA 19104

Cajetan Cordeiro
Air Products and Chemicals, Inc.
Allentown, PA 18195-1501

Abstract

The increasingly aggressive global competition for the production of higher quality polymer products at lower costs, along with a general trend away from new capital investments in the U.S., has placed considerable pressure on the process engineers in the U.S. to operate the existing polymer plants more efficiently and to use the same plant for the production of many different polymer products. The more efficient operation has been realized by better process control and monitoring while the available polymer product-quality sensors have been inadequate. Although many product quality indices cannot be measured readily, they can be estimated/inferred in real time from the readily available measurements, allowing for inferential control of the polymer product quality. This paper presents a survey of the issues in controlling and monitoring plant-product quality indices such as molecular weight, copolymer composition, and particle size distributions in polymerization reactors. Examples will be given to illustrate some of the methods surveyed.

Keywords

Particle size distribution, Process control, Inferential control, Batch control, Population balance models, Polymerization reactor control, Multi-rate measurements, Polymer product quality, Polymerization reactor monitoring

Introduction

A polymer product is composed of macromolecules with different molecular weights, and the processability and subsequent utility of a polymer product depends strongly on the macromolecule distributions, such as molecular weight distribution (MWD), copolymer composition distribution (CCD) [in copolymerization], and particle size distribution (PSD) [in emulsion polymerization]. For instance, in coatings, film formation, film strength, and gloss depend on the MWD, CCD, and PSD of the polymer. Since the distributions are influenced greatly by the polymerization reactor operating conditions, the production of a high quality polymer requires effective monitoring and control of the operating conditions (Congalidis and Richards, 1998; Ogunnaike, 1995). The effective monitoring and control can be realized only when sufficient frequent information on the distributions is available.

Polymerization reactors are a class of processes in which many essential process variables related to product quality cannot be measured or can be measured at low sampling rates and with significant time delays. The lack of readily-available, frequent measurements from which polymer properties can be inferred, has motivated a considerable research effort in the following research directions:

- The development of new on-line sensors [lists of many of the currently-available on-line sensors are provided in (Ray, 1986; Chien and Penlidis, 1990)].
- The development of qualitative and quantitative relations between easier-to-measure quality indices such as density, viscosity and refractive index, and more-difficult-to-measure quality indices such as conversion and average molecular weights (Kiparissides et al., 1980; Schork and Ray, 1983; Canegallo et al., 1993; Soroush and Kravaris, 1994; Ohshima et al., 1995; Ohshima and Tomita, 1995).
- The development of state estimators that are capable of estimating unmeasurable polymer properties from readily available measurements. The availability of sufficiently-accurate, first-principles, mathematical models of many polymerization reactors has made possible the development of reliable state estimators for the reactors (Jo and Bankoff, 1996; Ellis et al., 1988; Kim and Choi, 1991; Kozub and MacGregor, 1992; Ogunnaike, 1994).

Product Quality in Polymerization Processes

Product quality is a much more complex issue in polymerization than in more conventional short chain reactions (Ray, 1986). Because the molecular structure of the polymer is so sensitive to reactor operating conditions, upsets in feed conditions, mixing, reactor temperature and so on can change significantly critical molecular properties such as molecular weight distribution, copolymer composition distribution, copolymer chain sequence distribution, stereoregularity, and degree of chain branching.

The properties of a polymer product, such as the mechanical properties and the characteristics in molding, having strong correlation with the molecular weight distribution (MWD) of the polymer. Nunes et al. (1982) found that thermal properties, stress-strain properties, impact resistance, strength and hardness of films of polymethyl methacrylate and polystyrene were all improved

by narrowing MWD. It is also generally said that the polymer of long chain length gives superior mechanical properties to polymer products but has insufficient molding characteristics. Then the molding characteristics can be improved by blending short chain length polymer into this long chain length polymer, while the good mechanical characteristics are kept. That is, the broader MWD can be obtained by this blending. Therefore, the development of the methodology for adjusting MWD during the reaction to suitable one according to its use is desired, especially in producing high quality polymers.

Schoonbrood et al. (1995) studied the influence of copolymer composition and microstructure on the mechanical bulk properties of styrene-methyl acrylate copolymers. They found that copolymer composition drift has an influence on polymer mechanical properties such as Young's modulus, maximum stress, and elongation at break. In the case of copolymers that are homogeneous with respect to chemical composition, (a) maximum stress and elongation at break depend on the molecular weight distribution, (b) Young's modulus is independent of copolymer composition and molecular weight distribution in the ranges studied, and (c) maximum stress and elongation at break weakly depend on the copolymer composition. In the case of copolymers that are heterogeneous with respect to chemical composition, copolymer microstructure affects strongly Young's modulus, maximum stress, and elongation at break.

In paints and coatings, molecular weight, composition, and functional group distributions all play a key role in polymer performance. For solution viscosity reasons, narrow molecular weight distribution is useful, but not every paint or coating benefits from it. It depends on the application. For example, air-dry paints benefit from very broad molecular weight distribution (Grady, 2000).

For processing and end-use performance of latex coatings, it is often advantageous to produce a latex with high solids content while maintaining viscosity within acceptable limits. Latex particle size and particle size distribution directly affect the relationship between solids volume fraction and rheological properties. The influence of monodisperse latex particles on latex viscosity is described by the Dougherty-Krieger equation (Krieger and Dougherty, 1959),

$$\eta_r = \left(1 - \frac{\phi}{\phi_m}\right)^{-2.5\phi_m}$$

where η_r is the ratio of emulsion viscosity to that of the pure fluid (water for instance), ϕ is the volume fraction of solids, and ϕ_m is the maximum volume fraction of latex particles. For polydisperse systems, it has long been established that blends of different size particles yield viscosities which are lower than the viscosities of any of the monodisperse particles used to make nthe blend (for equivalent solids concentrations). Eveson and coworkers (1951) suggested that a particle suspension with a bimodal distribution can be regarded as a system in which the larger particles are suspended in a continuous phase formed by suspension of the smaller particles in the fluid medium. In other words, a suspension of smaller particles behaves essentially as a fluid toward the larger particles. Farris (1968) extended this line of reasoning to a multimodal blend of particle sizes with any number of modes and Parkinson et al. (1970) to a continuous particle size distribution. In both cases, successive application of a monodisperse expression for relative viscosity to particles of increasing size in a blend yielded an expression for relative viscosity of the form

$$\eta_r = \prod_i \left(1 - \frac{\phi_i}{\phi_{m,i}}\right)^{-k\phi_{m,i}}$$

where the ϕ_i are volume fractions of particles of a given size in the particle size distribution. Although this expressions is not directly applicable to the prediction of viscosity for continuous latex distributions, the reasoning behind its derivation suggests that control of the particle size distribution would be an appropriate approach to targeting desired latex rheological properties. In contrast, the more common approach of controlling moments of the distribution, is only indirectly related to target properties.

Classification of Variables in a Polymerization Plant

A customer evaluates the quality of a polymer product on the basis of indices, end-product quality indices, that are usually different from the product quality indices, plant-product quality indices, known to the plant process engineer. The end-product quality indices are related to the final use of the polymer product and usually cannot be measured in real time because of the complicated and slow measurement techniques needed or simply the inability to measure the quality indices until the final polymer product is formulated and used. On the other hand, polymer plants are operated at desired conditions by setting and regulating the plant variables (such as pressures, temperatures, and flow rates) that are measured readily on-line. We will refer to these readily measurable variables as basic plant variables to distinguish them from the plant-product quality indices and the end-product quality indices (end-use properties). These differences lead us to categorize variables in a polymer plant into the following three classes, intersections of which may not be null:

- Basic plant variables,
- Plant-product quality indices,
- End-product quality indices.

Basic plant variables that can be measured readily online and whose values are set by the process engineer to

operate the plant at desirable operating conditions. Examples of the basic process variables are temperatures, pressures, liquid levels, flow rates, and feed compositions.

Plant-product quality indices are usually monitored by the process engineer to ennnsure proper operation of the plant. Measurements of these indices are rarely available on-line and are usually obtained by laboratory sample analyses. Examples of these indices are viscosity, melt viscosity, density, copolymer composition distribution, molecular weight distribution, melt index, copolymer chain sequence distribution, stereoregularity, particle size distribution, porosity, surface area, and degree of chain branching.

End-product quality indices, often referred to as customer specifications or end-use properties, quantify the quality of the final product. These indices are usually "abstract" (to the plant process engineer), and their relations to the plant-product quality indices are complex and not well-understood. In many cases, the relations are known qualitatively on the basis of experience. It is important also to note that in cases where the relationships between these end-use properties and the plant-product quality indices are known, they are not "one-to-one". The end-product quality indices are rarely measured off-line in the plant because the measurements usually cannot be made until the final polymer product is formulated and used. Furthermore, many of these end-use properties (such as "softness", "blockiness", and "color") are "categorical" but not quantifiable in numerical form at the present time. Examples of the end-product quality indices (customer specifications) are adhesive strength, impact strength, hardness, elastic modulus, flow properties (film blowing, molding, etc.) strength, stress crack resistance, color, clarity, corrosion resistance, abrasion resistance, density, temperature stability, plasticity uptake, spray drying characteristics, and coating and adhesion properties. More examples of the end-product quality indices can be found in (Nunes et al., 1982; Ray, 1986; Dimitratos et al., 1994).

One of the greatest difficulties in achieving quality control of polymer end-products is our poor understanding of the quantitative relationship between (a) the end-product quality indices and (b) the plant-product quality indices and the basic plant variables. The actual customer specifications are in terms of the end-product quality indices. Since the quantitative relationship is the least understood area in polymerization reaction engineering, it is very hard to calculate the values of plant-product quality indices that corresponds to the actual customer specifications.

Mathematical Modeling

A major objective of polymerization reaction engineering has been to understand how reaction mechanism, the physical transport phenomena (e.g. mass and heat transfer, mixing), reactor type and operating conditions affect the plant-product quality indices. As discussed in (Ray, 1991), various chemical and physical phenomena occurring in a polymer reactor can be classified into the following three levels of modeling:

1. Microscale chemical kinetic modeling: Polymer reactions occur at the microscale. If the elementary reaction steps of a polymerization mechanism are known, the distributions can be calculated in terms of the kinetic rate constants and the concentration of the reactants. The available mathematical models are statistical or are based on detailed species conservation methods. The most powerful approach to modeling polymerization kinetics is the detailed species balance method. Using the conservation laws of mass, one can derive an infinite set of equations for the species present in the reaction mixture.
2. Mesoscale physical/transport modeling: At this scale, interphase heat and mass transfer, intraphase heat and mass transfer, interphase equilibrium, micromixing, polymer particle size distribution, and particle morphology play important roles and further influence the polymer properties. For example, diffusion-controlled free-radical polymerizations are manifestations of mesoscale mass transfer phenomena. For a comprehensive list of results available in this area, the reader can refer to the excellent review paper by (Kiparissides, 1996).
3. Macroscale dynamic reactor modeling: At the macroscale, one has to deal with the development of models describing the macromixing phenomena in the reactor, the overall mass and energy balances, particle population balances, the heat and mass transfer from the reactor as well as the reactor dynamics and control.

Population Balance Model

Population balance model descriptions have found a wide range of application in distributed process systems including crystallization, precipitation, and polymerization. An excellent treatment of the theoretical aspects of the subject is given in (Ramkrishna, 2000). In this paper, we focus on the application of population balance models to a specific sub-class of polymerization systems—particle size distributions in an emulsion system. Within this class, there are two general categories of behaviors: zero-one and pseudo-bulk systems. When conditions are such that the rate of radical-radical bimolecular termination within a latex particle is extremely fast relative to the rate of radical entry into particles, evolution of the latex particle size distribution can be modeled as a zero-one system (Gilbert, 1995). This model considers latex particles containing either zero or one radical at a given instant. The reasoning behind this model is that a particle will flip between two states, the zero and one

radical states, each time a radical enters the particle (or exits).

Latex particle size, monomer type and concentration, are among several key factors which strongly influence whether a system approaches zero-one kinetics. For example, termination of radicals within small particles is rapid because diffusion distance of the radical reaction centers is small. Moreover, radical entry rates, according to the Smoluchowski relation, $k_e = 4\pi r_s N_A D_w$ (r_s is swollen particle radius) decrease with decreasing particle size. In fact, many systems (styrene for example) approach zero-one kinetics during early stages of particle nucleation and growth when the size of particles is small.

To model a zero-one system, the particle size population is divided into a population containing zero radicals, $n_0(r)$ and a population containing one radical, $n_1(r)$. The one radical population is further divided into a population containing a polymer radical, $n_1(r)$, which would not readily diffuse out of the particle due to its size, and a population containing a monomer radical formed from chain transfer reactions, $n_1^m(r)$, which presumably can readily exit particles.

The population, $n_1(r)dr$, represents the moles(or number) of polymer particles per liter of water with unswollen particle radii between r and $r + dr$ at time t. Population balance equations for a batch reactor are given by:

$$\begin{aligned}\frac{\partial n_0(r,t)}{\partial t} &= \rho(r)\left[n_1(r) + n_1^m(r) - n_0(r)\right] + k_o(r)\cdot n_1^m(r) \\ &+ \int_{r_{nuc}}^{r/2^{1/3}} \frac{r^2 B(r-r',r')}{(r^3-r'^3)^{2/3}}\left[n_0(r')n_0(r-r') + \right. \\ &\qquad \left. n_1(r')n_1(r'-r)\right]dr' \\ &- n_0(r)\int_{r_{nuc}}^{r_\infty} B(r,r')\left[n_0(r') + n_1(r')\right]dr'\end{aligned}$$

$$\begin{aligned}\frac{\partial n_1(r,t)}{\partial t} &= \rho_{init}(r)\cdot n_0(r) \\ &- \rho(r)\cdot n_1(r) - k_{tr}C_p n_1(r) + k_p C_p n_1^m \\ &+ \int_{r_{nuc}}^{(r^3-r_{nuc}^3)^{1/3}} \frac{r^2 B(r-r',r')}{(r^3-r'^3)^{2/3}} n_0(r')n_1(r-r')dr' \\ &- n_1(r)\int_{r_{nuc}}^{r_\infty} B(r,r')\left[n_0(r') + n_1(r')\right]dr' \\ &- \frac{\partial}{\partial r}\left[G(r)\cdot n_1(r)\right] + \left[k^w_{p,j_{crit}-1}C_W\left[IM_{j_{crit}-1}\right]\right. \\ &\qquad \left. + \sum_{i=z}^{j_{crit}-1} k_{em,i}C_{micelle}\left[IM_i\right]\right]\delta(r-r_{nuc})\end{aligned}$$

Taking the first equation as an example, the terms premultiplied by $\rho(r)$ represent radical entry into particles, the next term represents radical desorption from particles, and the integral terms represent coagulation. The second equation has an additional term that represents new particle formation by micellular and homogeneous nucleation mechanisms.

Pseudo-bulk systems are characterized by slow radical termination within the particles relative to rapid entry of polymer radicals and re-entry of exited monomer radicals. In such systems, particles can contain more than one radical at a given instant. Moreover, particles with zero, 1, 2, ... radicals, switch identities(number of radicals) so rapidly that the evolution of the particle size distribution can be described by a single type of particle with an average number of radicals, $\bar{n}(r)$. Again, latex particle size, monomer type and concentration are factors which strongly influence whether a system approaches pseudo-bulk kinetics. Specifically, larger particle sizes increase radical entry rates and decrease radical termination and desorption rates, all of which favor pseudo-bulk kinetics.

The gel effect also decreases radical termination rates. This phenomenon is operative in many polymer systems when monomer concentration in particles is low relative to polymer concentration due to monomer depletion. Monomer depleted conditions often occur at the end of a batch when particle sizes are large. Therefore, the gel effect often coincides with large particle size and can be an additional factor which pushes a system towards pseudo-bulk kinetics.

A particle size distribution model for a pseudo-bulk system is given by:

$$\begin{aligned}\frac{\partial n(r,t)}{\partial t} &= \frac{1}{2}\int_{r_{nuc}}^{r-r_{nuc}} B(r-r',r')n(r')n(r-r')dr' \\ &- n(r)\int_{r_{nuc}}^{r_\infty} B(r,r')n(r')dr' - \frac{\partial}{\partial r}\left[G(r)\cdot n(r)\right] \\ &+ \left[k^w_{p,j_{crit}-1}C_W\left[IM_{j_{crit}-1}\right]\right. \\ &\qquad \left. + \sum_{i=z}^{j_{crit}-1} k_{em,i}C_{micelle}\left[IM_i\right]\right]\delta(r-r_{nuc})\end{aligned}$$

where particle growth rate is given by

$$G(r) = \frac{k_p C_p \bar{n}(r)\rho_p w_m}{4\pi r^2 N_a}$$

k_p is the propagation rate constant, C_p the monomer concentration in polymer particles, and $\bar{n}(r)$ the average radical concentration.

In summary, at least for a batch polymerization, zero-one kinetics is expected to be operative at early stages of polymerization when particle size is small and particles are rich in monomer whereas pseudo-bulk kinetics is favored in the latter stages of polymerization when particle size is large and the gel effect is strong. Of course neither of these models treats the more complicated intermediate case wherein particles can contain 0, 1, 2, and

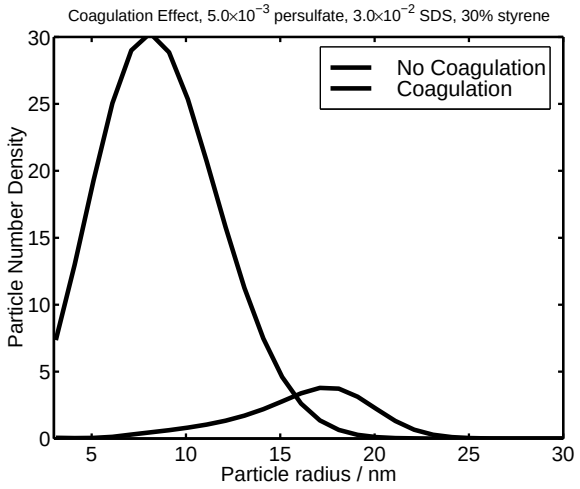

Figure 1: Simulation of zero-one model with and without coagulation 10 minutes after inception of polymerization.

3 radicals, for example, but for model based control purposes, we anticipate that the zero-one and pseudo-bulk models may be combined in a manner that adequately handles the intermediate case as well. Details of both these models can be found in (Gilbert, 1995).

Coagulation Coefficients. Coagulation is an extremely important phenomena in emulsion polymerization, having a large impact on latex particle numbers and particle size distributions. Actually, colloidal particles are thermodynamically unstable. Surface tension between particle and bulk phase dictates that free energy decreases upon particle coagulation due to decreased surface area (Atkins, 1978):

$$dG = \gamma dA$$
$$dG < 0 \qquad \text{for} \quad dA < 0$$

Colloidal stability is a consequence of kinetics. The electrostatic charge on the surface of a surfactant stabilized colloidal particle represents a significant energy barrier to coagulation between two approaching particles. If this barrier is large, very few particles will have sufficient kinetic energy to exceed the barrier and coagulate. Quantitatively, this potential energy barrier can be calculated using DLVO theory. This is based on calculating the total potential energy of interaction between two particles as the sum of a van der Waals attractive potential and an electrostatic repulsion potential (Ottewill, 1982). Details can be found in (Coen et al., 1998b) and the final result is

$$B(r_i, r_j) = \frac{2k_BT}{3\eta W_{ij}}\left(2 + \frac{r_{si}}{r_{sj}} + \frac{r_{sj}}{r_{si}}\right)$$
$$W_{ij} = \frac{r_{si} + r_{sj}}{4\kappa r_{si} r_{sj}} \exp\left(\frac{\Phi_{\max}}{k_BT}\right)$$

where W_{ij} is the Fuchs stability ratio and $\Phi_{\max}$ the maximum potential energy with respect to particle separation distance. One important characteristic of coagulation coefficients is that values increase exponentially as particle size is decreased. Also, for the smallest particles, the coagulation coefficient is nearly independent of the radius of the other particles with which the small particles coagulate. This feature was exploited for determining coagulation coefficients in our simulations by approximating the coagulation coefficients as depending only on the radius of the smaller of any two given particles coagulating. Figure 1 is a comparison of two simulated particle size distributions under identical operation conditions but with and without coagulation respectively. This figure highlights the influence that coagulation has on particle numbers and distributions during particle nucleation.

Calculation of coagulation coefficients in an on-line control application is problematic because calculation of $\Phi_{\max}$ is an extremum problem over particle separation distance and therefore, would be an embedded optimization problem. Another limitation of the DLVO theory is it does not account for shear effects which can markedly alter charge distributions surrounding particles and cause greatly accelerated coagulation rates. These problems are still open issues and feasible solutions will likely involve significant empiricism.

Numerical Solution

Approaches to solving population balance equations found in the literature can be generally classified into one of three distinct methods. Orthogonal collocation on fixed and moving finite elements has been used by several authors (Dafniotis, 1996; Rawlings and Ray, 1988a,b) to solve population balance models. This moving finite element method overcomes some of the numerical instabilities and inaccuracies associated with more conventional techniques such as finite differences.

Dafniotis (1996) describes the numerical problems associated with the solution of hyperbolic PDE's in terms of wave theory. If the desired solution is expressed in terms of a Fourier series, the behavior of a solution can be examined by examining individual components of the series, i.e., sine-cosine waves that propagate with specific phase and amplitude. Numerical operators such as finite differences, do not preserve the correct phase and amplitude. Particularly, errors associated with the phase are sometimes observed as spurious oscillations; referred to as dispersion. Also, when the amplitude of the numerical wave is damped relative to the exact solution

wave, discontinuities (for example boundary conditions) are smeared; referred to as numerical diffusion. Finally, hyperbolic partial differential equations often describe the propagation of near-shocks, or sharp wave fronts which require adequate resolution in the region of the shock.

In Dafniotis (1996), a moving finite element method(MFEM) is presented for solving the population balance equations for emulsion polymerization and to address some of the inherent numerical problems mentioned above. This method is based on the MFEM developed by Sereno and coworkers (1991).

A less sophisticated but much easier method to set up is the finite difference method. Here, partial derivatives in the population balance equations are approximated by finite differences. Gilbert (1997) has applied this method to modeling particle size distributions for emulsion polymerization systems.

A third method for solving population balance equations is sometimes referred to as methods of classes. Here, the distribution is discretized into classes of particles defined by finite particle size intervals. Mathematically, this involves transforming the partial differential equations from a differential to integrated form over small intervals. The presumed advantages of this approach include transformation of integral terms into more easily evaluated summation terms, elimination of partial differential terms with respect to particle size by forcing the discretization grid to move with particle growth rate, and the ability to coarsen the grid and still preserve key properties of the distribution such as moments (Kumar and Ramkrishna, 1996, 1997).

State Estimation

The inadequacy of frequent measurements related to the plant-product quality indices in polymer processes, has motivated the use of state estimators in controlling and monitoring the indices. The availability of sufficiently-accurate, first-principles, mathematical models for many polymerization reactors has made possible the development of the state estimators/observers. An estimator, which is designed on the basis of the process model, estimates unmeasured process variables from current and past process measurements. State estimators have also been used for sensor/plant fault detection and data reconciliation.

A major characteristic of polymerization reactors is their complex nonlinear behavior. Phenomena such as multiple steady states in continuouns stirred tank reactors, parametric sensitivity, and limit cycles are manifestations of the complex nonlinearity. Thus, reliable state estimation in polymerization reactors requires nonlinear models that can capture the complex nonlinear behavior. Motivated by the need for nonlinear state estimation, since the 1970s nonlinear state estimators have been used for polymerization reactors (Jo and Bankoff, 1996; Schuler and Suzhen, 1985; Ellis et al., 1988; Adebekun and Schork, 1989; Kim and Choi, 1991; Kozub and MacGregor, 1992; van Dootingh et al., 1992; Ogunnaike, 1994; Robertson et al., 1993; Liotta et al., 1997; Tatiraju et al., 1998a, 1999). In most of these studies, extended Kalman filters (EKF's) have been used for state estimation.

Multi-Rate State Estimation

In polymerization reactors, most of essential measurements related to plant-product quality indices, such as the leading moments of a MWD obtained by a gel permeation chromatograph (GPC), are available at low sampling rates and with considerable time-delays. On the other hand, measurements of basic plant variables such as temperatures, pressures, and densities are usually available at high sampling rates and with almost no delays. Because the plant product quality indices are usually not observable from the frequent, delay-free measurements alone, one has to design a multi-rate estimator/observer (i.e. one that uses both the frequent and infrequent measurements), to provide reliable estimates of the states, especially in the presence of model-plant mismatch and measurement noise. Multi-rate state estimation in polymerization processes has received considerable attention (Elicabe and Meira, 1988; Ellis et al., 1988; Dimitratos et al., 1989; Kim and Choi, 1991; Ogunnaike, 1994; Liotta et al., 1997; Mutha et al., 1997; Tatiraju et al., 1998a, 1999). Multi-rate EKF's have been used in most of these studies. For example, Ellis et al. (1988) used a multi-rate EKF to estimate the unmeasurable process states continuously from the frequently available measurements of temperature and density and the infrequent and delayed measurements of the average molecular weights (obtained by a gel permeation chromatograph). Mutha et al. (1997) proposed the use of a fixed-lag smoothing algorithm for multi-rate state estimation in a polymerization reactor. Tatiraju et al. (1998a, 1999) developed a method of multi-rate nonlinear state estimation and applied it to a solution polymerization reactor with fast measurements of reactor temperature, jacket temperature and density, and slow measurements of the zeroth, first and second moments of the polymer molecular weight distribution.

Inferential Control of Polymerization Reactors

An inferential control system has been defined conventionally as one that requires an estimated or inferred value of a controlled output to calculate the value of a manipulated input (Joseph and Brosilow, 1978a,b; Seborg et al., 1989; Marlin, 1995). Inferential control has application in processes in which (a) measurement of a controlled variable is not available frequently enough or

quickly enough to be used for feedback control, and (b) there are readily-available process measurements from which the value of the controlled variable can be inferred or estimated. The design of an inferential control system consists of two steps: (i) the synthesis of a controller assuming that all the controlled outputs are measured readily, and (ii) the design of an estimator to estimate the controlled outputs that are not measured readily. An inferential control system should ensure zero offset for all the controlled outputs. One of the industries that has benefitted greatly from inferential control is the polymer industry, where frequent measurements of even plant-product quality indices are rare. Extensive reviews of recent advances in inferential control can be found in (Doyle III, 1998; Soroush, 1998b).

Multi-Rate Control

In the polymer industry, there are many processes wherein the choice of sampling rate is limited by the availability of the output measurement. For example, composition analyzers such as gas chromatographs have a cycle time of say 5 to 10 minutes compared to a desired control interval of say 0.1 to 1 minute. If the control interval is increased to match the availability of measurements then control performance deteriorates significantly. In addition to the slow measurements (which are available at different low sampling rates and are delayed), there are usually process variables such as temperature and pressure that can be measured at high sampling rates and with almost no time delays, leading to multi-rate control problems. Successful recent implementations of multi-rate control on polymerization processes include (Ellis et al., 1994; Ogunnaike, 1994; Ohshima et al., 1994; Sriniwas et al., 1995; Crowley and Choi, 1996; Niemiec and Kravaris, 1997; Tatiraju et al., 1998b).

In the polymer industry, the problem of multi-rate control has been addressed by the following control methods:

- Cascade control
- Decentralized control
- State-estimator-based control

Cascade control systems have been used successfully to control essential variables whose measurements are not available frequently. The slave controller regulates a set of basic plant variables and adjust the manipulated inputs of process, while the master controller regulates the essential variables (usually plant-product quality indices) whose measurements are infrequent and delayed and calculates the set-points of the slave controller. While the inner loop is executed at the high rate at which the basic plant variables are measured, the outer loop is executed at the low rate at which the essential variables are measured (whenever these measurements are available). An advantage of this multi-rate control structure is its control system integrity in the face of any unforeseeable further delay in the essential slow measurements; whether the slow measurements arrive or not, the inner loop is always in place (Lee and Morari, 1990; Lee et al., 1992).

Decentralized control systems have been used in the polymer industry to control process variables whose measurements are available at different rates. As in every decentralized control system design, first the manipulated inputs and the controlled outputs should be paired. A single-input single-output controller is then designed for each pair. Each of the SISO controllers is executed (takes action) at the rate at which the measurements of the corresponding controlled output are available. An advantage of these multi-rate control structures is also its control system integrity in the face of any unforeseeable further delay in the slow measurements; whether the slow measurements arrive or not, the "fast" loops are always in place.

State-estimator-based multi-rate control systems include a state estimator which estimates frequently all state variables of the process from the available, fast and slow measurements. The frequent measurements and estimates are then fed to a single-rate controller as if the process has only single-rate measurements. In contrast to the first two classes of the multi-rate control systems that can be non-model-based, the last class of the multi-rate systems have to be model-based (since they include estimators).

Batch Control Issues

Model-based Optimization Approaches to Batch Polymerization Control

In the case of batch systems, one can formulate a classical optimal control problem in an effort to control the endpoint properties of the batch. In a number of studies, this is implemented in a receding horizon framework, yielding a so-called Model Predictive Controller (MPC). MPC utilizes a process model to compute a future open-loop control sequence which optimizes an objective function, given past and current information of the system. The first control move is implemented and the optimization problem is re-solved at the next sampling time as updated information becomes available.

Applications of MPC to semi-batch polymerization systems include (Russell et al., 1997), where *linear* MPC was applied to a Nylon system using empirical models for quality control. The primary modification to the MPC algorithm was the use of a shrinking horizon, originally proposed in (Joseph and Hanratty, 1993). A similar formulation of MPC was adopted by Georgakis and co-workers (Liotta et al., 1997). In their work, a *nonlinear* formulation was proposed; however, they employed a "least-squares"-like analytical solution to the unconstrained problem. Another notable citation is the work

in (Ettedgui et al., 1997), where a fed-batch reactor is studied (in simulation) for the application of nonlinear model-based estimation and predictive control. In that case, the sequential solution and optimization technique of (Wright and Edgar, 1994) was employed.

In general, MPC is posed as an on-line optimization problem, typically requiring the solution of a constrained linear, quadratic, or nonlinear programming problem. The generalized optimization problem considered can be expressed as:

$$\min_{\underline{u}}[\max \Phi_i(\underline{x},\underline{u})] \qquad i = 1, n_{obj}$$

subject to

$$\begin{aligned} \dot{\underline{x}} &= f(\underline{x},\underline{u}) \\ g_i(\underline{u}) &\le 0 \qquad i = 1, n_{ineq} \\ h_i(\underline{u}) &= 0 \qquad i = 1, n_{eq} \end{aligned}$$

Here, the vector $\underline{u}$ contains the values for the sequence of manipulated variable moves over the batch cycle (*e.g.*, surfactant feed), n_{obj} denotes the number of terms considered in the objective function, and the constraints describe the process model and corresponding operating constraints. Several forms of the objective function can be considered. The following 1-norm type objective could be considered:

$$\Phi = \sum_{i=1}^{N_E}\sum_{j=1}^{N_J} \frac{\left|n_{ij} - n_{ij}^{target}\right|}{n_{scale}}$$

Here, n_{scale} is a factor used to scale the objective function values. A 2-norm objective can also be formulated;

$$\Phi = \sum_{i=1}^{N_E}\sum_{j=1}^{N_J} \left[\frac{(n_{ij} - n_{ij}^{target})}{n_{scale}}\right]^2$$

Many interesting polymer products have corresponding distributions that are multi-modal in nature. These can be produced, for example, by multiple surfactant additions, sufficiently separated in time. Therefore, a potentially effective objective definition is to actually define multiple objective functions, each tied to a particular distribution mode, and perform a min-max optimization. For bimodal distributions, the objective can be expressed as follows:

$$\Phi_1 = \sum_{i=1}^{N_1}\sum_{j=1}^{N_J} \left[\frac{(n_{ij} - n_{ij}^{target})}{n_{scale}}\right]^2$$

$$\Phi_2 = \sum_{i=N_1+1}^{N_E}\sum_{j=1}^{N_J} \left[\frac{(n_{ij} - n_{ij}^{target})}{n_{scale}}\right]^2$$

$$\min_{u_i, i=1,11} \Phi = \max(\Phi_1, \Phi_2)$$

Here, N_1 represents the number of finite elements spanning the lower particle size mode of the distribution.

Case Study I: Control of an Emulsion Polymerization Reactor

The control of particle size distribution as an end-objective in emulsion polymerization control is well motivated in industrial practice, and has been well documented in the literature (see, for example, the recent review by Congalidis and Richards, 1998). The authors pointed out that "on-line control not only of average polymer properties but also of polymer distributions such as the particle size... will become important". They continue: "The instrumentation and control methodologies that will need be deployed to meet these needs is a challenging and vibrant area of investigation for academic researchers and industrial practitioners alike."

In this section, we present a case study for the optimal control of particle size distribution in a semi-batch styrene polymerization reactor. The isothermal model of Coen et al. (1998a) incorporates current theory on particle nucleation, growth and coalescence mechanisms for styrene at $50°C$ and serves as the modeling basis for this study. This model is a *zero-one* model, referring to the assumption of instantaneous bimolecular radical termination in polymer particles, which gives rise to a mixed population of particles containing either one or zero radicals. Parts of the model that deviate from (Coen et al., 1998a) are described in detail in (Crowley et al., 2000).

The basic control problem is defined as the achievement of a target PSD at the end of the batch. For this study, we consider the manipulation of both surfactant feed rate (and/or concentration), and initiator feed rate. On-line measurement of the full PSD, for example by light scattering, is assumed for this study.

Open-loop Optimization of PSD

Two distinct variables related to surfactant concentrations were optimized to match a target PSD. The first variable considered is surfactant feed rate. Specifically, the optimization routine calculates a sequence of 10 surfactant feed flow rates(zero-order hold), each with a sample hold time of 3 minutes, up to a final time of 30 minutes. The target PSD was generated by simulating the model up to 30 minutes, with values for the 10 surfactant feed flow rates that yield a bimodal distribution. Control trajectories were calculated by defining an objective function in terms of simulated PSD deviations from a target distribution, and minimizing the objective function using the sequential quadratic programming algorithm, FSQP.

In a different approach, we considered use of free surfactant concentration, rather than surfactant feed rate, as the control variable. The reason behind this choice is that free surfactant concentration above the cmc is the essential driving force for particle nucleation. The free surfactant profiles consist of a sequence of first-order holds (i.e. piecewise linear), with each hold spanning a 3

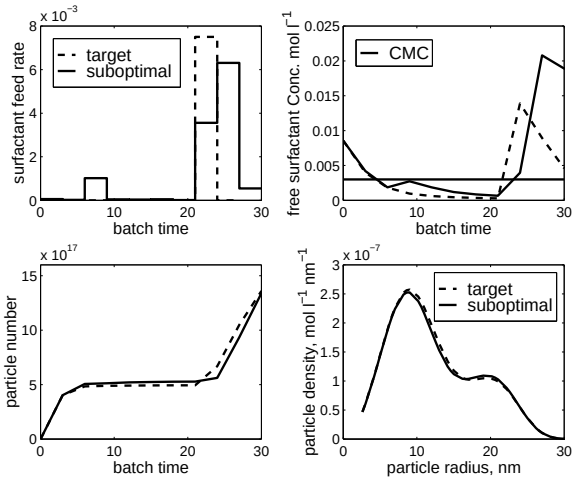

Figure 2: Optimization of surfactant feed rate sequence for target PSD; cmc= 3×10^{-3} mol/L, $[I]_0 =$ 0.01 mol/L, $[M]_0 = 2.59$ mol/L.

minute interval. As in the previous case, 10 holds were used to span a 30 minute control horizon. For this formulation of the optimization problem, the decision variables are 11 free surfactant concentration nodes, spaced at 3 minute intervals. Free surfactant concentration values between any two neighboring nodes are calculated simply by linear interpolation between the two nodal values. Linked in this way, the nodes form a continuous, though non-smooth, free surfactant profile.

The first optimization case involves computation of a sequence of surfactant feed flow rates which drive the system to a target PSD. The target distribution was generated by fixing the initial surfactant concentration at time= 0 and simulating the system out to 30 minutes with one large surfactant addition at 21 minutes. This addition is shown in Figure 2. Surfactant addition at 21 minutes produces a shoulder in the distribution at the end of the 30 minute simulation, with a peak height located at a particle size of about 20 nm. The solid stair case profile for surfactant feed rate in this figure represents the optimization solution. The 2-norm objective was used in this case. Although the optimizer appears to drive the simulated PSD to the target, as seen in this figure, the final free surfactant concentration for the optimized case is much larger than that of the target case. With disparity in surfactant levels at 30 minutes, the two distributions would diverge beyond this time. These differences can be improved through the use of input blocking (Crowley et al., 2000).

The optimal solution is quite sensitive to the choice of initial conditions, as well as the particular blocking formulation. Consequently, a second control strategy was considered. Because particle nucleation is dependent on the free surfactant level relative to the critical micelle concentration, a free surfactant trajectory is more closely related to the physical phenomena than surfactant feed flow rates. Of course, ultimately the feed flow rates are manipulated. A free surfactant trajectory represents a higher control level in a cascade configuration, with feed rates being the lowest level control variable. A useful property arises from this form. An intuitive initialization for optimization computations is to set all free surfactant concentrations in the control vector to the critical micelle concentration. Sensitivity of particle nucleation rate to surfactant perturbations is greatest at the CMC.

Local minima are often a cause of poor performance in gradient based optimization. For a bimodal distribution, it is possible to obtain suboptimal PSD solutions that are trapped in a local minimum because surfactant perturbations which decrease target offset for one of the modes may increase offset for the other mode. As an attempt to partially decouple this kind of interaction, we formulated a multi-function objective wherein each function is tied to a particular mode of the distribution. As described above, the resulting optimization is a min-max problem with two objective functions for a bimodal distribution. Figure 3 depicts the result of this case. When compared to the PSD offsets seen using the 2-norm (Crowley et al., 2000), the target offset for the min-max optimization is lower. Another advantage of this approach is that the optimization is "well-behaved" in the sense that offset of each mode from the target is balanced due to the structure of the objective function.

Batch-to-Batch Studies

In this section, a model refinement optimization technique is described using information from historical batch data of emulsion polymerization in conjunction with a fundamental first-principles model to determine the operating conditions necessary for a desired product quality.

The desired product quality must be a grade of product produced in the same range of operating conditions used in the historical batch data. As a result of this condition, the desired PSD must have a similar character to known PSDs produced by the process. A fundamental first-principles model of emulsion polymerization which accounts for polymer particle nucleation and polymer propagation exists. While these phenomena are well understood, emulsion polymerization presents a challenging process to control due to difficulty in modeling complex behavior such as particle aggregation and the significant nonlinear behavior involved in particle formation. The method described in this section seeks to combine this first-principles model of emulsion polymerization with an MPLS model to find the optimal control input sequence needed to achieve a desired product quality in a semi-batch emulsion polymerization reaction. In the experiments conducted in this section, the process variables are the surfactant and initiator feed rate inputs at distinct

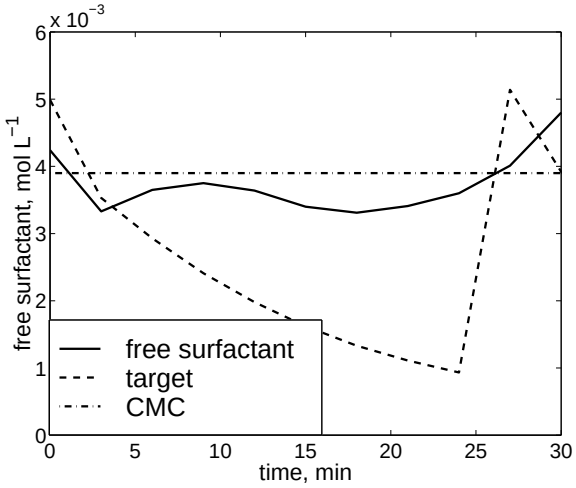

(a) Free surfactant profiles.

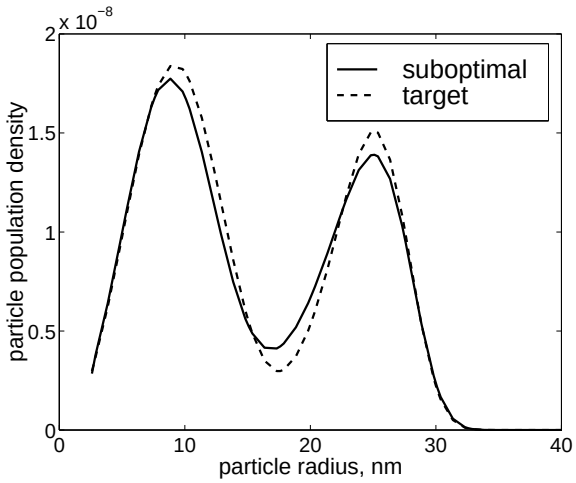

(b) Particle size distributions.

Figure 3: Synthesis of optimal free surfactant profile using min-max objective. Target and suboptimal distributions shown are at a batch time of 30 minutes. Initial reactant conditions are as follows: cmc= 0.0039, $[I]_0 = 0.005$ mol/L, $[M]_0 = 2.59$ mol/L.

time intervals, and the product quality is determined by the particle size distribution (PSD) at the final time of the experiment.

The design of inputs for the emulsion polymerization process is performed on an off-line batch-to-batch basis. The hybrid model, which combines a first-principles model with MPLS, is referred to as the design model. The MPLS model is used to approximate the difference between the PSD the first-principles model calculates and the PSD obtained from executing a given input sequence in an actual semi-batch reactor, thus capturing the effect of phenomena for which the first-principles model does not take into account. The optimization will be performed by minimizing the sum of the squared residual error between the PSD yielded by the design model and the target PSD. The design model is a function of the states of the system and the control inputs. A calibration set of data from historical batches having a set of operating conditions similar to that of the desired PSD will be required to begin the optimization procedure. The PSDs in the historical batch data and the target PSD are created from a virtual process model which simulates the actual semi-batch reaction in a plant. This virtual process model is structurally different from the first-principles model in the design model because it accounts for aggregation and has four parameter values that are varied from the design model values by 5%.

The hybrid design model is potentially useful because the MPLS model will account for the phenomena such as particle aggregation which are not included in the first-principles model within the design model. Furthermore, the MPLS model can be adjusted to account for noise that may occur during PSD measurement. In addition, the MPLS model calibration set can be refined once a significant amount of batches have been designed by using only a subset of historical batches in the MPLS model, and including only those batches most recently designed. A pure MPLS model could also be attempted, but important information can be extracted from the first-principles model, so one would not want to abandon it altogether. The first-principles model in the design model could be useful for optimizing control inputs for new processes with little batch history, and for optimizing control inputs for new grades with no batch history. The efficacy of using a first-principles/MPLS hybrid model in achieving a target PSD is investigated in the following work.

While MPCA is used to compress information in the process variables to low-dimensional spaces that describe the historical batch operation, MPLS reduces both the process variables and product quality variables to low dimensional spaces, and attempts to find a correlation between these low-dimensional spaces (Neogi and Schlags, 1998). PLS attempts to maximize covariance, which means that it focuses on the variance of X that is more predictive for the product quality Y, rather than focusing on the variance of X only (Nomikos and MacGregor, 1995). In this investigation, the MATLAB PLS Toolbox 2.0 by Eigenvector, Inc is used to perform PLS analyses.

Before beginning the optimization algorithm, it is necessary to generate historic batch data and a target PSD with the use of the process model. The target PSD must

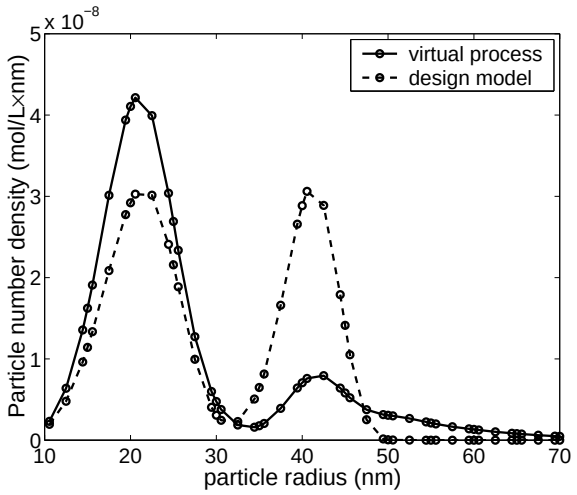

Figure 4: PSD for virtual process and design model.

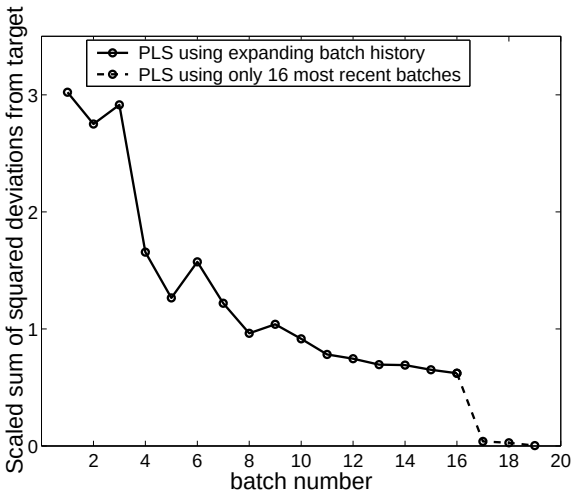

Figure 5: Improvement of PSD tracking error over the course of 20 successive batches.

be created within the same range of operating conditions used to generate the batch history, so that it is a different grade of product, within the same product family. The target PSD and historic PSDs are vectors containing the 48 particle number densities yi corresponding to 48 discrete particle radii r_i . A control input sequence of length 20 corresponding to the surfactant and initiator feed inputs at 10 evenly spaced time steps for a 100 minute batch reaction are used to create the PSDs.

The first step in the optimization algorithm is to obtain the scaling data and PLS regression matrix for the current batch history (X and Y blocks) in MATLAB.

The second step in the optimization is to design an input sequence using the following hybrid design model:

$$y^{design}(t = t_f) = y^{fp}(x, u, t) + y^{resid}(x, u)$$

where

$$y^{fp}(x, u, t_f) = \int_0^{t_f} f(x, u)dt$$

In this equation, t_f is the duration time of the semi-batch reaction, x and u are vectors containing the states of the system and the control inputs of the system, respectively y^{resid} is an approximation of the residual PSD between the process model PSD and the PSD from the first-principles model. $y^{resid}(x, u)$is calculated using the regression matrix calculated with the current batch history. The first iteration of the optimization will require an initial value for the control input sequence u. The optimization is performed by making small perturbations in u for each iteration. The direction of the perturbations are determined by the Jacobian matrix calculated from the previous iteration of the optimization. The size of the perturbation in u is fixed prior to optimization. The following objective function is minimized by the optimization procedure to determine control input sequence u to be used in the next batch:

$$\sum_{i=1}^{n_y} \left(y_i^{target} - y_i^{design}\right)^2$$

The optimized input sequence is then executed in the virtual process model, which simulates a batch reaction within an actual plant. Representative results of this study are shown below in Figures 4 and 5. The first figure shows the mismatch between the simulated process and the fundamental model used for PSD control. The overall trend along the batch history is mapped in the form of integral squared error in Figure 5. Clearly, the algorithm "learns" as the batches proceed.

Case Study II: Control of a Solution Polymerization Reactor

In this section, we present a comparative study of multi-rate control of a jacketed polymerization reactor in which free-radical solution polymerization of styrene takes place. A multi-rate control system consisting of the multi-rate nonlinear state estimator of (Tatiraju et al., 1999) and a mixed error- and state-feedback controller, is used. The performance of the multi-rate nonlinear control system is shown and compared with those of a multi-rate, PI, parallel cascade, control system and a multi-rate, PI, completely decentralized, control system.

Polymerization Process and the Control Problem

The reactor is a 3 m^3, jacketed, continuous, stirred tank reactor in which free-radical solution polymerization of styrene takes place. The solvent and initiator are benzene and azo-bis-iso-butyro-nitrile, respectively. The reactor has three feed streams: a pure monomer stream

at a volumetric flow rate of F_m, a pure solvent stream at a volumetric flow rate of F_s, and an initiator stream, which includes solvent and initiator, at a volumetric flow rate of F_i. The volume of the reacting mixture inside the reactor is constant.

We use the same dynamic model described in (Tatiraju et al., 1999) to represent the reactor. The model has the form:

$$\begin{aligned}
\frac{dC_i}{dt} &= -\left[\frac{F_t}{V} + k_i\right] C_i + \frac{F_i C_{i_i}}{V} \\
\frac{dC_s}{dt} &= -\frac{F_t C_s}{V} + \frac{F_i C_{s_i} + F_s C_{s_s}}{V} \\
\frac{d\lambda_0}{dt} &= -\frac{F_t \lambda_0}{V} + f_3(C_i, C_s, C_m, T) \\
\frac{d\lambda_1}{dt} &= -\frac{F_t \lambda_1}{V} + f_4(C_i, C_s, C_m, T) \\
\frac{d\lambda_2}{dt} &= -\frac{F_t \lambda_2}{V} + f_5(C_i, C_s, C_m, T) \\
\frac{dC_m}{dt} &= f_6(C_i, C_m, T) + \frac{F_m C_{m_m} - F_t C_m}{V} \\
\frac{dT}{dt} &= f_7(C_i, C_m, T, T_j) + \frac{F_t(T_{in} - T)}{V} \\
\frac{dT_j}{dt} &= f_8(T, T_j) + \alpha Q
\end{aligned} \tag{1}$$

where $F_t = F_i + F_m + F_s$, V is the volume of the reacting mixture inside the reactor, C_m is concentration of the monomer in the reactor outlet stream, C_i is concentration of the initiator in the reactor outlet stream, C_s is concentration of the solvent in the reactor outlet stream, T is the reactor temperature, T_j is the jacket temperature, Q is the rate of heat input to the reactor jacket, and λ_0, λ_1 and λ_2 are the zeroth, first, and second moments of the MWD of the polymer product, respectively. The functions $f_1, \cdots, f_8$ and the parameter values of the reactor model are given in (Tatiraju et al., 1999); for brevity they are not given here. The first-principles mathematical model of the process described by (1) is used to represent the actual process.

The number-average and weight-average molecular weights of the polymer product (denoted by M_n and M_w respectively) are related to the moments according to

$$M_n = \frac{\lambda_1}{\lambda_0}, \qquad M_w = \frac{\lambda_2}{\lambda_1}$$

The reacting mixture density, reactor temperature (T), and jacket temperature (T_j) are assumed to be measured on-line once every 30 seconds and with almost no time delays. The monomer conversion (and thereby the monomer concentration, C_m) can be inferred from the density measurement, and thus can be calculated on-line. The zeroth, first, and second moments of the MWD of the polymer product are assumed to be measured at sampling periods of 3 hours and with time delays of 1 hour. The rate of heat input to the reactor jacket, Q, and the flow rate of the initiator feed stream, F_i, can be set arbitrarily on-line within the following ranges: $-20 \le Q \le 50 \;\; kJ.s^{-1}$ and $0 \le F_i \le 3.0 \times 10^{-5} \;\; m^3.s^{-1}$.

The control problem is to maintain the weight-average molecular weight of the polymer, M_w, and the reactor temperature, T, at desired values by manipulating the rate of heat input to the reactor jacket, Q, and the flow rate of the initiator feed stream, F_i.

Multi-Rate Nonlinear Control System

State Feedback Synthesis. With M_w and T as controlled outputs ($y_1 = M_w$ and $y_2 = T$), and F_i and Q as manipulated inputs ($u_1 = F_i$ and $u_2 = Q$), relative orders (degrees) of the process $r_1 = 2$ and $r_2 = 1$, and the characteristic (decoupling) matrix of the process is generically singular. Because of this generic singularity, we request a state feedback that induces two completely decoupled, 2nd-order, process output responses of the form:

$$\beta_{12}\frac{d^2 M_w}{dt^2} + \beta_{11}\frac{dM_w}{dt} + M_w = M_{w_{sp}} \tag{2}$$

$$\beta_{22}\frac{d^2 T}{dt^2} + \beta_{21}\frac{dT}{dt} + T = T_{sp} \tag{3}$$

where β_{12}, β_{11}, β_{22} and β_{21} are positive adjustable scalar parameters, $M_{w_{sp}}$ is the weight-average molecular weight set-point, and T_{sp} is the reactor temperature set-point. Substituting for the time derivatives from the process model in the preceding two equations, we obtain two identities of the forms

$$\begin{aligned}
\phi_1(x, u_1) &= \frac{1}{\beta_{12}} M_{w_{sp}}, \\
\phi_2(x, u_1, u_2, \dot{u}_1) &= \frac{1}{\beta_{22}} T_{sp}
\end{aligned} \tag{4}$$

where x is the vector of the state variables of the reactor. Let us represent the solution for $u = [u_1 \;\; u_2]^T$ of the constrained minimization problem

$$\min_u \left\{ \left[\phi_1(x, u_1) - \frac{M_{w_{sp}}}{\beta_{12}}\right]^2 + \left[\phi_2(x, u_1, u_2, 0) - \frac{T_{sp}}{\beta_{22}}\right]^2 \right\}$$

subject to

$$\begin{aligned}
0 \le u_1 \le 3.0 \times 10^{-5} \;\; m^3.s^{-1} \\
-20 \le u_2 \le 50 \;\; kJ.s^{-1},
\end{aligned}$$

by

$$u = \Psi(x, M_{w_{sp}}, T_{sp}) \tag{5}$$

Using the identities of (4), we add integral action to the state feedback of (5) (see Soroush, 1998a, for the details),

leading to the mixed error- and state-feedback controller

$$\begin{aligned}
\dot{\eta}_1 &= \eta_2 \\
\dot{\eta}_2 &= -\frac{1}{\beta_{12}}\eta_1 - \frac{\beta_{11}}{\beta_{12}}\eta_2 + \phi_1(x, u_1) \\
\dot{\eta}_3 &= \eta_4 \\
\dot{\eta}_4 &= -\frac{1}{\beta_{22}}\eta_2 - \frac{\beta_{21}}{\beta_{22}}\eta_4 + \phi_2(x, u_1, u_2, 0) \\
u &= \Psi(x, e_1 + \eta_1, e_2 + \eta_3)
\end{aligned} \tag{6}$$

where $e_1 = M_{w_{sp}} - M_w$ and $e_2 = T_{sp} - T$. The controller of (6) has integral action and inherently includes optimal windup and directionality compensators (Soroush, 1998a).

Multi-Rate State Observer. Application of the multi-rate nonlinear state estimation method described in (Tatiraju et al., 1999) to this polymerization reactor leads to the following reduced-order, multi-rate, nonlinear, state estimator:

$$\begin{bmatrix} \dot{z}_1 \\ \dot{z}_2 \\ \dot{z}_3 \\ \dot{z}_4 \\ \dot{z}_5 \end{bmatrix} = \begin{bmatrix} -\left[\frac{F_t}{V} + k_i\right]\hat{C}_i + \frac{F_i C_{i_i}}{V} \\ -\frac{F_t \hat{C}_s}{V} + \frac{F_i C_{s_i} + F_s C_{s_s}}{V} \\ -\frac{F_t \hat{\lambda}_0}{V} + f_3(\hat{C}_i, \hat{C}_s, C_m, T) \\ -\frac{F_t \hat{\lambda}_1}{V} + f_4(\hat{C}_i, \hat{C}_s, C_m, T) \\ -\frac{F_t \hat{\lambda}_2}{V} + f_5(\hat{C}_i, \hat{C}_s, C_m, T) \end{bmatrix}$$
$$- K \begin{bmatrix} f_6(\hat{C}_i, C_m, T) + \gamma_1 \\ f_7(\hat{C}_i, C_m, T, T_j) + \gamma_2 \\ f_8(T, T_j) + \alpha Q \end{bmatrix} + L \begin{bmatrix} \lambda_0^* - \hat{\lambda}_0 \\ \lambda_1^* - \hat{\lambda}_1 \\ \lambda_2^* - \hat{\lambda}_2 \end{bmatrix} \tag{7}$$

$$\begin{aligned}
\hat{C}_i &= z_1 + K_{11} C_m + K_{12} T + K_{13} T_j \\
\hat{C}_s &= z_2 + K_{21} C_m + K_{22} T + K_{23} T_j \\
\hat{\lambda}_0 &= z_3 + K_{31} C_m + K_{32} T + K_{33} T_j \\
\hat{\lambda}_1 &= z_4 + K_{41} C_m + K_{42} T + K_{43} T_j \\
\hat{\lambda}_2 &= z_5 + K_{51} C_m + K_{52} T + K_{53} T_j
\end{aligned}$$

where $L = [L_{ij}]$ and $K = [K_{ij}]$ are the estimator gains,

$$\gamma_1 = \frac{F_m C_{m_m} - (F_i + F_m + F_s) C_m}{V}$$

$$\gamma_2 = \frac{(F_i + F_m + F_s)(T_{in} - T)}{V}$$

$\lambda_0^*(t)$, $\lambda_1^*(t)$ and $\lambda_2^*(t)$ are the predicted present values of the infrequent measurable outputs, each of which is obtained by fitting a least-squared-error line to the most recent, three measurements of the moment. These linear regressions are always carried out except when only one measurement of each slow measurable output is available. In this case, the predicted present value of each slow measurable output is set equal to the single available measurement. The estimator initial conditions are the same as those in (Tatiraju et al., 1999). The multi-rate state estimator of (7) can be written in the compact form

$$\begin{aligned}
\dot{z} &= F(z, \tilde{y}, Y^*, u) \\
\hat{x} &= Q(z, \tilde{y})
\end{aligned} \tag{8}$$

where $Y^* = [\lambda_0^* \ \lambda_1^* \ \lambda_2^*]^T$ and $\tilde{y} = [C_m \ T \ T_j]^T$.

Multi-Rate Nonlinear Control System. The use of the mixed error- and state-feedback controller of (6), together with the multi-rate state estimator of (7), leads to a multi-rate nonlinear control system of the form:

$$\begin{aligned}
\dot{z} &= F(z, \tilde{y}, Y^*, u) \\
\dot{\eta}_1 &= \eta_2 \\
\dot{\eta}_2 &= -\frac{1}{\beta_{12}}\eta_1 - \frac{\beta_{11}}{\beta_{12}}\eta_2 + \phi_1(\hat{x}, u_1) \\
\dot{\eta}_3 &= \eta_4 \\
\dot{\eta}_4 &= -\frac{1}{\beta_{22}}\eta_2 - \frac{\beta_{21}}{\beta_{22}}\eta_4 + \phi_2(\hat{x}, u_1, u_2, 0) \\
u &= \Psi(\hat{x}, \tilde{e}_1 + \eta_1, e_2 + \eta_3) \\
\hat{x} &= Q(z, \tilde{y})
\end{aligned} \tag{9}$$

where $\tilde{e}_1 = M_{w_{sp}} - \hat{\lambda}_2/\hat{\lambda}_1$.

Multi-Rate Cascade and Decentralized Control Systems

We compare the performance of the multi-rate nonlinear control system of (9) with a multi-rate, PI, cascade, control system and a multi-rate, PI, completely decentralized, control system.

The multi-rate, PI, cascade, control system consists of two PI controllers. The master PI controller regulates the weight-average molecular weight by manipulating the reactor temperature set-point. The master controller is executed once every three hours, since the average molecular weight measurements are available at that low rate. The slave PI controller regulates the reactor temperature by manipulating the rate of heat input to the reactor jacket. The slave controller is executed at a much faster rate (once every 30 seconds). The control system has the form

$$\begin{aligned}
\xi_1(k+1) &= \left[1 - \frac{\Delta t}{\tau_{I_1}}\right]\xi_1(k) + \frac{\Delta t}{k_{c_1}}\left[T_{sp}(k) - T_{sp_{ss}}\right] \\
\dot{\xi}_2(t) &= -\frac{1}{\tau_{I_2}}\xi_2(t) + \frac{1}{k_{c_2}}\left[Q(t) - Q_{ss}\right] \\
T_{sp}(k) &= \mathrm{sat}_T\left\{T_{sp_{ss}} + k_{c_1}\left[\bar{e}_1(k) + \frac{1}{\tau_{I_1}}\xi_1(k)\right]\right\} \\
Q(t) &= \mathrm{sat}_Q\left\{Q_{ss} + k_{c_2}\left[\bar{e}_2(t) + \frac{1}{\tau_{I_2}}\xi_2(t)\right]\right\}
\end{aligned} \tag{10}$$

with $\xi_1(0) = M_w(0)$, $\xi_2(0) = T(0)$, $k_{c_1} = -4.0 \times 10^{-5}$, $k_{c_2} = 1.0 \times 10^{-4}$, $\tau_{I_1} = 1.0 \times 10^6$ s, and $\tau_{I_2} = 1.0 \times 10^6$ s, where $\bar{e}_1(k) = M_{w_{sp}}(t) - M_w(k)$, $\bar{e}_2(t) = T_{sp}(t) - T(t)$, and $\Delta t = 1.08 \times 10^4$ s.

The multi-rate, PI, completely decentralized, control system consists of two completely-decentralized PI controllers. One of the PI controllers regulates the weight-average molecular weight by manipulating the flow rate of the initiator feed stream, and the other regulates the reactor temperature by manipulating the rate of heat input to the reactor jacket. While the first PI controller is executed once every three hours (sampling rate of the average molecular weight), the second controller is executed once every 30 seconds (sampling rate of the reactor temperature). The control system has the form

$$\begin{aligned} \xi_1(k+1) &= \left[1 - \frac{\Delta t}{\tau_{I_1}}\right] \xi_1(k) + \frac{\Delta t}{k_{c_1}} \left[F_i(k) - F_{i_{ss}}\right] \\ F_i(k) &= \text{sat}_{F_i} \left\{ F_{i_{ss}} + k_{c_1} \left[\bar{e}_1(k) + \frac{1}{\tau_{I_1}} \xi_1(k) \right] \right\} \\ \dot{\xi}_2(t) &= -\frac{1}{\tau_{I_2}} \xi_2(t) + \frac{1}{k_{c_2}} \left[Q(t) - Q_{ss}\right], \\ Q(t) &= \text{sat}_Q \left\{ Q_{ss} + k_{c_2} \left[\bar{e}_2(t) + \frac{1}{\tau_{I_2}} \xi_2(t) \right] \right\} \end{aligned} \tag{11}$$

with $\xi_1(0) = M_w(0)$, $\xi_2(0) = T(0)$, $k_{c_1} = -5.0 \times 10^{-7}$, $k_{c_2} = 2.5 \times 10^{-4}$, $\tau_{I_1} = 1.0 \times 10^7$ s, and $\tau_{I_2} = 1.0 \times 10^6$ s.

Each of the preceding PI control systems includes two PI controllers with windup compensators (Soroush, 1998a).

Simulation Results

The performance of the multi-rate nonlinear controller is evaluated by simulating the following two cases: (a) when there is no measurement noise or model-plant mismatch (nominal case); and (b) when there are measurement noise and model-plant mismatch (non-nominal case). For each case, the performance of the multi-rate nonlinear control (NC) system is compared with those of the cascade control (CC) system and the decentralized control (DC) system. Measurement noise is introduced by adding a white noise signal to each of the moments calculated by the process model. Each of the noise signals is a 10% deviation from the value of the moment at that particular time. Model error is simulated by adding a 10% error in the propagation step rate constant. The following values of tunable parameters are used for the nonlinear controller:

$$K_{11} = 1.0, \quad K_{12} = 0.0, \qquad K_{13} = 1.0$$

$$K_{i1} = K_{i2} = K_{i3} = 0.0, \qquad i = 2, \ldots, 5,$$

$$L_{i1} = L_{i2} = L_{i3} = 0.0, \qquad i = 1, \ldots, 2$$

$$L_{ij} = 0.0, \qquad i \neq j,\ i = 3, \ldots, 5;\ j = 1, \ldots, 3$$

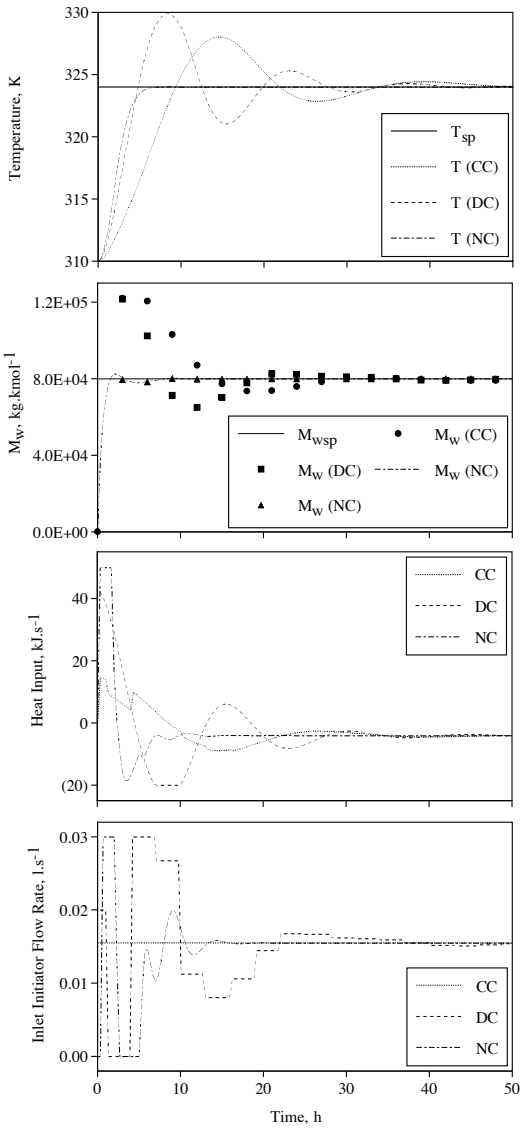

Figure 6: Controlled outputs and manipulated inputs under the multi-rate control systems (nominal case).

The temperature set-point $T_{sp} = 324.0$ K, and the weight-average molecular weight set-point $M_{w_{sp}} = 80{,}000$ $kg.kmol^{-1}$.

Figure 6 shows the profiles of the controlled outputs and the manipulated inputs for the nominal case under the three multi-rate control systems. The solid line represents the set point. For the M_w graph, the dashed line stands for the continuous estimates of M_w obtained by using the estimator of the multi-rate NC system, while the bullets stand for the infrequent and delayed "measurements" of the average-molecular weight. For this case, $L_{31} = 1.0 \times 10^{-4}, L_{42} = 1.0 \times 10^{-9}$, and $L_{53} = 1.0 \times 10^{-8}$. The benefit of using the multi-rate

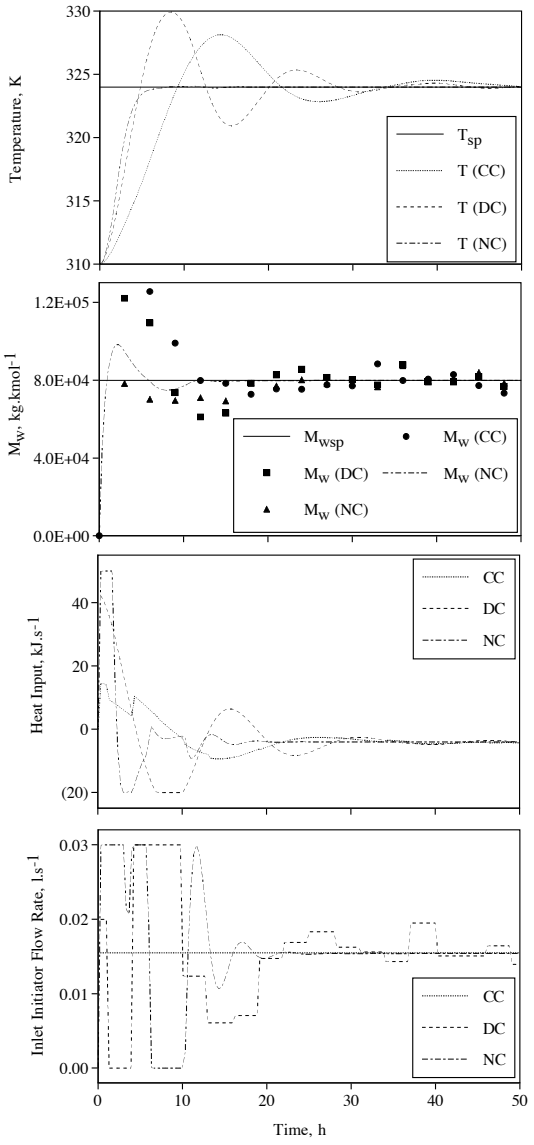

Figure 7: Controlled outputs and manipulated inputs under the multi-rate control systems (non-nominal case).

NC system is obvious in Figure 6. Not only under the NC system are the process output responses faster, but also they have smaller overshoots in the controlled variables. Under the CC and DC systems it takes more than 40 hours to take both the temperature and average molecular weight to their respective set-points, while under the NC system it takes less than 5 hours. The CC system regulates M_w only by manipulating Q, but the DC system regulates both M_w and T by manipulating Q and F_i. From the manipulated input graphs we can see that the NC system makes the most optimal use of manipulated variables. Under the CC and DC systems the manipulated inputs hardly reach the constraints, but still the CC and DC systems cannot be tuned to be more aggressive because the overshoots start increasing. Figure 7 depicts the profiles of controlled outputs and manipulated inputs for the non-nominal case. For this case, $L_{31} = 1.0\times10^{-4}$, $L_{42} = 2.0\times10^{-7}$, and $L_{53} = 9.5\times10^{-6}$. Again, the NC system shows a much superior performance as compared to the two PI control systems.

Conclusions

In this paper a brief survery of the recent advances that have led to improvement in polymer product quality was presented. Further improvement in polymer product quality requires solving challenging design, control, and monitoring problems that still exist in polymer processes.

Lack of sufficient controllability is a barrier to better product quality control in some polymer processes. In many polymer processes, better product quality requires minimizing/maximizing several product quality indices simultaneously. This multi-objective requirement may result in narrow ranges of process trajectories, putting a premium on the controllability of the process. For instance, in coatings, the product's composition, molecular weight, and particle size distributions should be maintained simultaneously in limited ranges to ensure the coating has a desired level of film formation, film strength, and gloss.

In many batch processes, product quality suffers from batch-to-batch inconsistency. There is a trend towards products with specific performance, which have higher value to a formulator or end-user. Furthermore, many of the current processes result in products with a broad inter-batch variance of molecular and physical characteristics, which in turn result in broad variance of performance. Blending of these batches usually lowers the average performance of the product lots. Segregation of "off-spec" product results in higher costs which may not be transferable to the customer.

Our understanding of the relationships among the basic plant variables, plant-product quality indices, and end-product quality indices is mostly empirical and qualitative. Polymer product development in the absence of qualitative relationships between the recipe, process and the final performance requires long times. Experimental techniques have been used to develop relationships that hold for the range of the experimental parameters studied. These products and processes therefore do not readily lend themselves to optimization, either in terms of productivity or reduction in variance. Having the ability to develop these relationships on a more fundamental basis will allow products to be developed in shorter times.

Acknowledgments

Financial support from the National Science Foundation through the grant CTS-9703278 is gratefully acknowledged by M. Soroush. The first author would like to acknowledge the financial support of NSF (BES 9896061) as well as the valuable contributions to this work by Tim Crowley, Charles Immanuel, and Chris Harrison.

References

Adebekun, D. K. and F. J. Schork, "Continuous Solution Polymerization Reactor Control 2: Estimation and Nonlinear Reference Control during Methyl Methacrylate Polymerization," *Ind. Eng. Chem. Res.*, **28**, 1846 (1989).

Atkins, P. W., *Physical Chemistry*. W. H. Freeman, second edition edition (1978).

Canegallo, S., G. Storti, M. Morbidelli, and S. Carra, "Densitometry for On-line Conversion Monitoring in Emulsion Homo- and Co-polymerization," *J. App. Poly. Sci.*, **47**, 961 (1993).

Chien, D. C. H. and A. Penlidis, "On-line Sensors for Polymerization Reactors," *JMS-Rev. Macromol. Chem. Phys.*, **C30(1)**, 1 (1990).

Coen, E. M., R. G. Gilbert, B. R. Morrison, H. Leube, and S. Peach, "Modeling particle size distributions and secondary particle formation in emulsion polymerisation," *Polymer*, **39**(26), 7099–7112 (1998a).

Coen, E. M., R. G. Gilbert, B. R. Morrison, H. Leube, and S. Peach, "Modelling particle size distributions and secondary particle formation in emulsion polymerisation," *Polymer*, **39**(26), 7099–7112 (1998b).

Congalidis, J. P. and J. R. Richards, "Process Control of Polymerization Reactors: An Industrial Perspective," *Polymer Reaction Eng.*, **6**(2), 71–111 (1998).

Crowley, T. J. and K. Choi, "On-line Monitoring and Control of a Batch Polymerization Reactor," *J. Proc. Cont.*, **6**, 119 (1996).

Crowley, T. J., E. S. Meadows, E. Kostoulas, and F. J. Doyle III, "Control of Particle Size Distribution Described by a Population Balance Model of Semibatch Emulsion Polymerization," *J. Proc. Cont.*, **10**, 419–432 (2000).

Dafniotis, P., *Modelling of emulsion copolymerization reactors operating below the critical micelle concentration*, PhD thesis, University of Wisconsin-Madision (1996).

Dimitratos, J., C. Georgakis, M. S. El-Aasser, and A. Klein, "Dynamic Modeling and State Estimation for an Emulsion Copolymerization Reactor," *Comput. Chem. Eng.*, **13**(1/2), 21–33 (1989).

Dimitratos, J., G. Elicabe, and C. Georgakis, "Control of Emulsion Polymerization Reactors," *AIChE J.*, **40**(12), 1993–2021 (1994).

Doyle III, F. J., "Nonlinear Inferential Control for Process Applications," *J. Proc. Cont.*, **8**, 339–353 (1998).

Elicabe, G. E. and G. R. Meira, "Estimation and Control in Polymerization Reactors. a Review," *Poly. Eng. & Sci.*, **28**, 121 (1988).

Ellis, M., T. W. Taylor, V. Gonzalez, and K. F. Jensen, "Estimation of the Molecular Weight Distribution in Batch Polymerization," *AIChE J.*, **34**, 1341–1353 (1988).

Ellis, M. F., T. W. Taylor, V. Gonzalez, and K. F. Jensen, "Estimation of the Molecular Weight Distribution in Batch Polymerization," *AIChE J.*, **34**, 1341 (1994).

Ettedgui, B., M. Cabassud, M.-V. Le Lann, N. L. Ricker, and G. Casamatta, NMPC-based Thermal Regulation of a Fed-Batch Chemical Reactor Incorporating Parameter Estimation, In *IFAC Symposium on Advanced Control of Chemical Processes*, pages 365–370, Banff, Canada (1997).

Evenson, G. F., S. G. Ward, and R. L. Whitmore, "Theory of size distributions: Paints, coals, greases,etc. Anomalous viscosity in model suspensions," *Discussions f the Faraday Society*, **11**, 11–14 (1951).

Farris, R. J., "Prediction of the viscosity of multimodel suspensions from unimodal viscosity data," *Trans. Soc. Rheology*, **12**(2), 281–301 (1968).

Gilbert, R. G., *Emulsion polymerization: a mechanistic approach*. Academic Press (1995).

Gilbert, R. G., Modelling Rates and Molar Mass Distributions, In Lovell, P. A. and M. S. El-Aasser, editors, *Emulsion Polymerization and Emulsion Polymers*, chapter 5, pages 165–203. John Wiley and Sons (1997).

Grady, M., Personal communication (2000).

Jo, J. H. and S. G. Bankoff, "Digital Monitoring and Estimation of Polymerization Reactors," *AIChE J.*, **22**, 361 (1996).

Joseph, B. and C. B. Brosilow, "Inferential Control of Processes: 1. Steady State Analysis and Design," *AIChE J.*, **24**, 485–492 (1978a).

Joseph, B. and C. B. Brosilow, "Inferential Control of Processes: 3. Construction of Optimal and Suboptimal Dynamic Estimators," *AIChE J.*, **24**, 500–509 (1978b).

Joseph, B. and F. W. Hanratty, "Predictive Control of Quality in a Batch Manufacturing Process Using Artificial Neural Networks," *Ind. Eng. Chem. Res.*, pages 1951–1961 (1993).

Kim, K. J. and K. Y. Choi, "On-line Estimation and Control of a Continuous Stirred Tank Polymerization Reactor," *J. Proc. Cont.*, **1**, 96 (1991).

Kiparissides, C., J. F. MacGregor, S. Singh, and A. E. Hamielec, "Continuous Emulsion Polymerization of Vinyl Acetate. Part III: Detection of Reactor Performance by Turbidity Spectra and Liquid Exclusion Chromatography," *Can. J. Chem. Eng.*, **58**, 65 (1980).

Kiparissides, C., "Polymerization Reactor Modeling: a Review of Recent Developments and Future Directions," *Chem. Eng. Sci.*, **51**, 1637 (1996).

Kozub, D. J. and J. F. MacGregor, "State Estimation for Semi-Batch Polymerization Reactors," *Chem. Eng. Sci.*, **47**, 1047–1062 (1992).

Krieger, I. M. and T. J. Dougherty, "A mechanism for non-Newtonian flow in suspensions of rigid spheres," *Trans. Soc. Rheology*, **3**, 137 (1959).

Kumar, S. and D. Ramkrishna, "On the solutions of population balance equations by discretization—I. A fixed pivot technique," *Chem. Eng. Sci.*, **51**(8), 1311–1332 (1996).

Kumar, S. and D. Ramkrishna, "On the solution of population balance equations by discretization–III. Nucleation, growth and aggregation of particles," *Comput. Chem. Eng.*, **52**(24), 4659–4679 (1997).

Lee, J. H. and M. Morari, "Robust Inferential Control of Multi-rate Sampled-data Systems," *Chem. Eng. Sci.*, **47**, 865 (1990).

Lee, J. H., M. S. Gelormino, and M. Morari, "Model Predictive Control of Multi-Rate Sampled-Data Systems: A State-Space Approach," *Int. J. Control*, **55**(1), 153–191 (1992).

Liotta, V., C. Georgakis, and M. S. El-Aasser, Real-time Estimation and Control of Particle Size in Semi-Batch Emulsion Polymerization, In *Proc. American Control Conf.*, pages 1172–1176, Albuquerque, NM (1997).

Marlin, T. E., *Process Control: Designing Processes and Control Systems for Dynamic Performance*. McGraw-Hill, Inc. (1995).

Mutha, R. K., W. R. Cluett, and A. Penlidis, "On-Line Nonlinear Model-Based Estimation and Control of a Polymer Reactor," *AIChE J.*, **43**(11), 3042–3058 (1997).

Neogi, D. and C. E. Schlags, "Multivariable statistical analysis of an emulsion batch process," *Ind. Eng. Chem. Res.*, **37**, 3971–3979 (1998).

Niemiec, M. and C. Kravaris, Nonlinear Multirate Model Algorithmic Control and its Application to a Polymerization Reactor, In *AIChE Annual Meeting* (1997).

Nomikos, P. and J. F. MacGregor, "Multi-way partial least squares in monitoring batch processes," *Chemometr. Intell. Lab.*, **30**, 97–108 (1995).

Nunes, R. W., J. R. Martin, and J. F. Johnson, "Influence of Molecular Weight and Molecular Weight Distribution on Mechanical Properties of Polymers," *Poly. Eng. & Sci.*, **4**, 205 (1982).

Ogunnaike, B. A., "On-Line Modelling and Predictive Control of an Industrial Terpolymerization Reactor," *Int. J. Control*, **59**(3), 711–729 (1994).

Ogunnaike, B. A., A Contemporary Industrial Perspective on Process Control Theory and Practicce, In *DYCORD '95* (1995).

Ohshima, M. and S. Tomita, Model-based and Neural-net-based On-line Quality Inference System for Polymerization Processes, In *AIChE Annual Meeting* (1995).

Ohshima, M., I. Hashimoto, H. Ohno, M. Takeda, T. Yoneyama, and F. Gotoh, "Multirate Multivariable Model Predictive Control and its Application to a Polymerization Reactor," *Int. J. Control*, **59**, 731 (1994).

Ohshima, M., A. Koulouris, S. Tomita, and G. Stephanopoulos, Wave-Net Based On-Line Quality Inference System for Polymerization Processes, In *4th IFAC Symposium on Dynamics and Control of Chemical Reactors, Distillation Columns and Batch Processes*, page 275 (1995).

Ottewill, R. H., *The stability and instability of polymer latices*, chapter 1. Academic Press (1982).

Parkinson, C., S. Masumoto, and P. Sherman, "The influence of particle-size distribution on the apparent viscosity of non-newtonian dispersed systems," *J. Colloid and Interface Sci.*, **33**(1), 151–161 (1970).

Ramkrishna, D., *Population Balances*. Academic Press, San Diego (2000).

Rawlings, J. B. and W. H. Ray, "The Modeling of Batch and Continuous Emulsion Polymerization Reactors. Part I: Model Formulation and Sensitivity to Parameters," *Poly. Eng. Sci.*, **28**, 237–256 (1988a).

Rawlings, J. B. and W. H. Ray, "The Modeling of Batch and Continuous Emulsion Polymerization Reactors. Part II: Comparison With Experimental Data From Continuous Stirred Tank Reactors," *Poly. Eng. Sci.*, **28**, 257–274 (1988b).

Ray, W. H., "Polymerization Reactor Control," *IEEE Cont. Sys. Mag.*, **6**((4)S), 3–8 (1986).

Ray, W. H., "Modeling of Addition Polymerization Processes—Free Radical, Ionic, Group Transfer, and Ziegler-Natta Kinetics," *Can. J. Chem. Eng.*, **69**, 626 (1991).

Robertson, D. G., P. Kesavan, and J. H. Lee, Detection and Estimation of Randomly Occurring Deterministic Disturbances, In *Proc. American Control Conf.*, page 4453, Seattle, WA (1993).

Russell, S. A., P. Kesavan, J. H. Lee, and B. A. Ogunnaike, Recursive Data-Based Prediction and Control of Product Quality for Batch and Semi-batch Processes Applied to a Nylon 6,6 Autoclave, In *AIChE Annual Meeting, paper no. 196* (1997).

Schoonbrood, H. A. S., H. M. G. Brouns, H. A. Thijssen, A. M. van Herk, and L. German, "The Effect of Composition Drift and Copolymer Microstructure on Mechanical Bulk Properties of Styrene-Methyl Acrylate Emulsion Copolymers," *Macromol. Symp.*, **92**, 133 (1995).

Schork, F. J. and W. H. Ray, "On-line Measurement of Surface Tension and Density with Application to Emulsion Polymerization," *J. Appl. Poly. Sci.*, **25**, 407 (1983).

Schuler, H. and Z. Suzhen, "Real-time Estimation of Chain Length Distribution in a Polymerization Reactor," *Chem. Eng. Sci.*, **40**, 1891 (1985).

Seborg, D. E., T. F. Edgar, and D. A. Mellichamp, *Process Dynamics and Control*. John Wiley and Sons, Inc., New York, NY (1989).

Sereno, C., A. Rodrigues, and J. Villadsen, "The moving finite element method with polynomial approximation of any degree," *Comput. Chem. Eng.*, **15**(1), 25–33 (1991).

Soroush, M. and C. Kravaris, "Nonlinear Control of a Polymerization CSTR with Singular Characteristic Matrix," *AIChE J.*, **40**, 980 (1994).

Soroush, M., Directionality and Windup Compensation in Nonlinear Model-Based Control, In Berber, R. and C. Kravaris, editors, *Nonlinear Model-Based Process Control*, volume 353 of *NATO ASI Series E*, page 173. Kluwer Academic Publishers, Dordrecht (1998a).

Soroush, M., "State and Parameter Estimations and their Applications in Process Control," *Comput. Chem. Eng.*, **23**, 229–245 (1998b).

Sriniwas, G. R., Y. Arkun, and F. J. Schork, "Estimation and Control of an Alpha-olefin Polymerization Reactor," *J. Proc. Cont.*, **5**, 303 (1995).

Tatiraju, S., N. Zambare, M. Soroush, and B. A. Ogunnaike, Multirate Control of a Polymerization Reactor, In *AIChE Spring Meeting* (1998b).

Tatiraju, S., M. Soroush, and B. A. Ogunnaike, Multi-Rate Nonlinear State Estimation in a Polymerization Reactor, In *Proc. American Control Conf.*, page 3165, Philadelphia, PA (1998a).

Tatiraju, S., M. Soroush, and B. Ogunnaike, "Multi-rate Nonlinear State Estimation with Application to a Polymerization Reactor," *AIChE J.*, **45**(4), 769 (1999).

van Dootingh, M., F. Viel, D. Rakotopara, J. P. Gauthier, and P. Hobbes, "Nonlinear deterministic observer for state estimation: Application to a continuous free radical polymerization reactor," *Comput. Chem. Eng.*, **16**, 777–791 (1992).

Wright, G. T. and T. F. Edgar, "Nonlinear Model Predictive Control of a Fixed-Bed Water-Gas Shift Reactor: An Experimental Study," *Comput. Chem. Eng.*, **18**(2), 83–102 (1994).